CHAPTER 13

Piezoelectric Composite Materials

13.1 Introduction

A *piezoelectric composite* is a combination of a piezoelectric ceramic and/or a polymer and a nonpiezoelectric polymer constituting a new version of piezoelectric material. In general terms, piezoelectric composite applies to any piezoelectric material resulting from combining a piezoelectric polymer or ceramic with other nonpiezoelectric materials including air-filled voids. Figure 13.1 illustrates different ways of constituting a piezoelectric composite material.

Earlier versions of piezoelectric composites synthesized include barium titanate embedded polymer matrix and lead zirconate-titanate (PZT) ceramic powder dispersed in a polymeric receptacle. Subsequent developments are: (i) Flexible piezoelectric composites using $PbTiO_3$ or PZT plus synthetic rubber; (ii) PVDF-based pyroelectric composites; (iii) woven PZT ceramic/polymer composites; and (iv) calcium modified lead titanate rods embedded in a polymer matrix. The development of piezoelectric composites was motivated by the efforts to find a class of piezoelectric materials which offer substantial improvements over the conventional piezoelectric ceramics and polymers for making ultrasonic transducers used in medical imaging and for hydrophone applications.

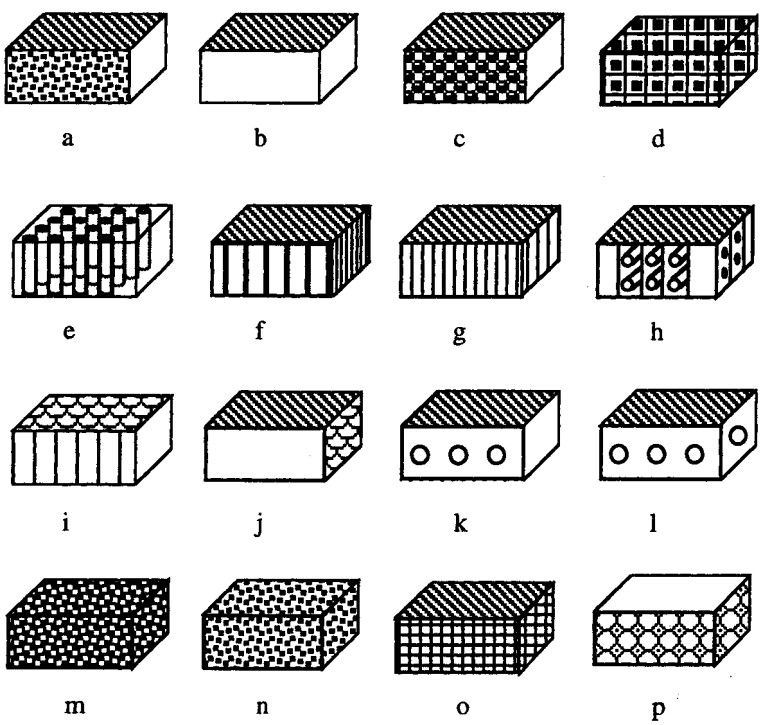

Figure 13.1 Different types of piezoelectric composites [6].
(a) Particles in a polymer: 0-3; (b) PVDF composite: 0-3; (c) PZT spheres in a polymer: 1-3; (d) diced composite: 1-3; (e) PZT rods in a polymer: 1-3; (f) sandwich composite: 1-3; (g) glass-ceramic composite: 1-3; (h) transverse reinforced composite: 1-2-0; (i) honeycomb composite: 3-1P; (j) honeycomb composite: 3-1S; (k) perforated composite: 3-1; (l) perforated composite 3-2; (m) replamine composite: 3-3; (n) burps composite: 3-3; (o) sandwich composite: 3-3; (p) ladder-structured composite: 3-3.

Combining a piezoelectric ceramic and a passive polymer to form a piezoelectric composite facilitates transducer designs that offer several advantages over the use of conventional piezoelectric ceramics or polymers. For example, the rod composite geometry (Figure 13.2) allows enhanced electroelastic coupling and permits designs of transducers with adequate impedance matching feasibilities. Likewise, the dice-and-fill technique (Figure 13.3) adopted in constituting a piezoelectric composite allows shaped geometries of the transducers facilitating focused ultrasonic beams. Further, judicious rod spacing in the composite yields materials with low cross-talk between array elements.

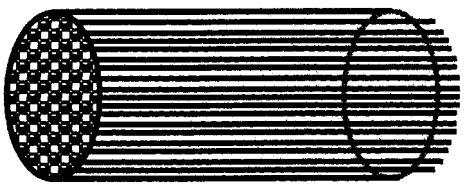

Figure 13.2 Rod piezoelectric composite (Example: PZT rods in a polymer).

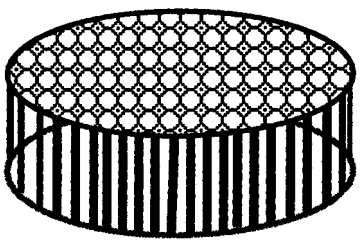

Figure 13.3 Dice-and-fill composite.

Existing studies [1-12] address the various trial-based synthesis of piezoelectric composites with different constituent materials, measurement of the electroelastic properties of the test composites, application of the piezoelectric composites and analytical endeavors to formulate the effective electroelastic parameters of the composite. In the following sections descriptions of various composites are developed; their fabricational aspects, functional characteristics, application potentials and a summary of the theoretical considerations are presented.

13.2 Connectivity-Based Structured Piezoelectric Composites

To understand how different versions of piezoelectric composites are constituted, it is necessary to define a critical parameter, namely, the *connectivity* which refers to the manner or the pattern in which the diphasic or multiphasic constituents are self-connected in zero, one, two or three dimensions. Denoting the connectivity as AB, (A = B $\in$ 0, 1, 2, 3), the zero depicts the total absence of linkage between the particulates. That is, the particles of a given constituent remain discrete and isolated totally delinked from the other particles. When the particles are connected across one, two, or three dimensionally, the corresponding designations are 1, 2, and 3, respectively. Thus, for diphasic constituents, the designation 02, for example, means that one of the materials has particles which are discretely isolated and delinked from each other; and the other material has particulate dispersion with the formation of chain links in two dimensions. Sketched in Figure 13.4 are cubical representations of self-connected systems.

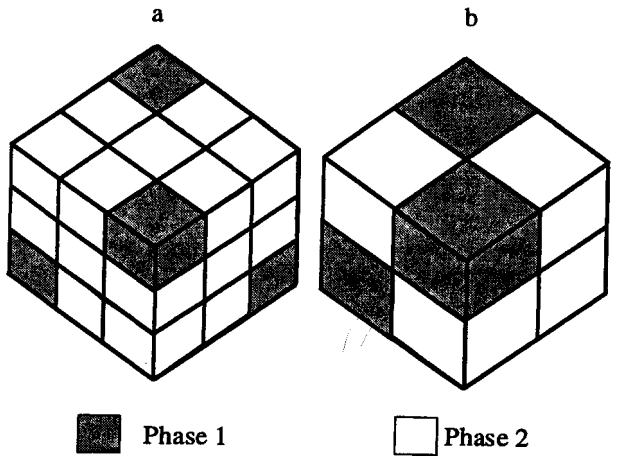

Figure 13.4 Cubic representation of a self-connected diaphasic system. (a) Volume fraction of phase 1 is smaller than the volume fraction of phase 2; (b) Both phases have equal volume fractions.

In view of the self-connecting arrangements of the diphasic constituents, practical structuring of piezoelectric composites is manifold and the schematic diagrams of such various types of structured piezoelectric composites are depicted in Figure 13.5.

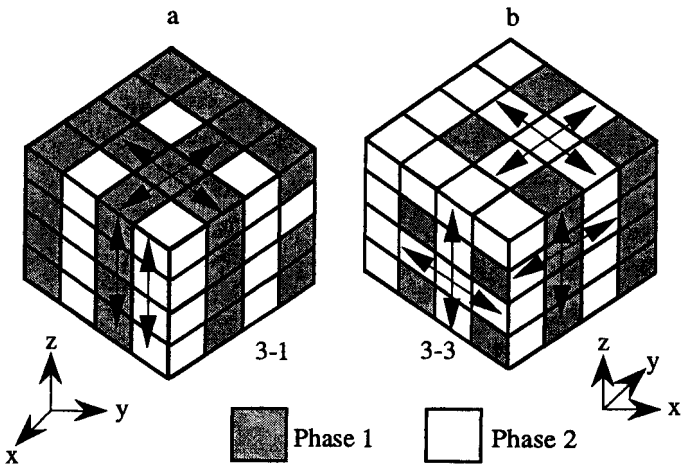

Figure 13.5 Two typical connectivity patterns for a diphasic system. Examples: (a) In the 3-1 composite the shaded phase is three-dimensionally connected and the unshaded phase is one-dimensionally connected. (b) Composite 3-3 shows connectivity pattern. (A set of ten connectivity patterns are illustrated in [11].)

13.3 Fabricational Considerations

13.3.1 *Rod composites*: One of the most popular piezoelectric composites refers to "PZT rods in a polymer" with 1-3 connectivity. It has been identified as a promising element for medical ultrasonic transducer applications. The rod composites are fabricated as follows:

- Slender rods of a piezoelectric ceramic (such as PZT) are aligned in a parallel stack, a polymer is cast between them, and the desired composite link is sliced off (Figure

13.2). The above method is effective for making samples with rod diameters about 200 microns or more. Finer spatial scales are difficult to achieve due to the handling of delicate ceramic rods.

- For spatial scales below 50 microns, a large number of carbon fibers are woven into the desired structure by textile methods and the carbon structure is replicated with piezoelectric ceramic.

- Alternatively, a complementary structure is formed in plastic, and a ceramic slip is injected into this mold and fixed. The plastic mold burns away during the firing, and a polymer is cast back into its place (*lost wax method*). This method yields large area, low cost composites.

- *Dice-and-fill technique*: Figure 13.3 illustrates a widely spread fabrication method for piezoelectric composites. Deep grooves are cut into a solid ceramic and a polymer is cast into these grooves. The resulting composite disk is then sliced off the ceramic base. The dicing operation is feasible for rod dimensions down to 50 microns. Finer spatial scales are possible *via* laser machining to cut the grooves. Laser-induced etching and/or laser ablation may permit scale sizes as low as 10 microns. The dice-and-fill technique is devoid of rod-fragility problems. However, machining and polishing of brittle ceramic and soft polymer combinations may pose engineering problems. Temperature problems and polymer shrinkage effects are other technology factors associated with this method of fabrication.

- *Lamination technique:* Alternate plates of piezoelectric ceramic and a passive material are glued to form a layered stack. Slicing perpendicular to this stack yields a composite thin loaf with 1-3 connectivity. The passive material could be nonpolymeric as well. (Figure 13.6)

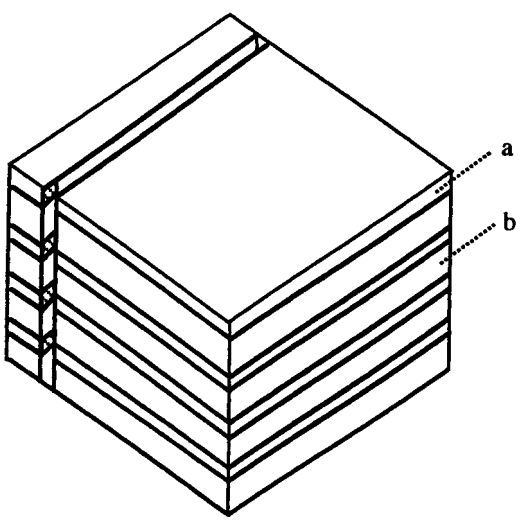

Figure 13.6 Lamination-type composite.
(a) Piezoelectric plate; (b) passive material; (c) a sliced part.

13.4 Flexible Composite Fabrication

Typical flexible composites are :

(a) Gould flexible composite: 5 to 10 μm piezoelectric particles embedded in a polyurethane matrix

(b) Honeywell (T-flex)™ composite: 120 μm piezoelectric composites embedded in a silicone rubber matrix

(c) Honeywell's large-sized piezoelectric embed in a host silicone rubber matrix

In polymer-based flexible composites, the low permittivity polymer layer normally interleaves the piezoelectric particles preventing saturation poling, after the composite is formed. When the piezoelectric particulate bridges the electrodes, it eliminates the poling problem. However, the performance of the composite is controlled by particulate position.

The fabrication procedure involves mixing the piezoelectric ceramic particles (typically Bi_3O_3-modified $PbTiO_3$ or WO_3-modified $Pb(Zr,Ti)O_3$ and synthetic rubber (or chloroprene rubber) and rolling down about 0.5 mm thick sheets at 40°C using a hot roller; and then it is heated at 190°C for 20 minutes under pressure of 30 kg/cm^2. The conductive paste (Fujikura Chemical, Dotite D500™) is attached on both sides of the sheet as electrodes. The specimens are polarized at 60°C in silicone oil by applying a DC field of 100 kV/cm for 1 hour.

Another example of flexible piezoelectric composites is: NTK piezo-rubber™ (NTK Technical Ceramic Division, Japan). It consists of $PbTiO_3$ ceramic powder in chloroprene rubber matrix. It is available in piezo-rubber sheet form and/or as piezo-rubber wire form [12].

Woven PZT ceramic/polymer composite: A *replication process (replamineform process)* is used to fabricate woven PZT/polymer composites. Fabric templates consisting of woven carbon fibers are impregnated with PZT by soaking it in a solution containing stoichiometric amounts of dissolved lead, zirconium, titanium, and niobium. Subsequent heat treatment burns out the carbon, leavning a PZT replica with the same form as the initial carbon weave. To form a composite, replicas are sintered in a controlled atmosphere and backfilled with epoxy polymer. This process has been attempted with as-received activated and non-activated carbon fabrics, as well as those fabrics pretreated with hydrogen peroxide.

Constituting a 3-3 composite by replication process should characterize the end product ideally with the following features: (i) A narrow pore-size distribution; (ii) pore volume closely equal to solid-phase volume; and, (iii) complete pore interconnectivity.

Table 13.1 Characteristics of Piezoelectric Materials

Poled Piezoelectric Materials	Piezoelectric Coefficient 10^{-12} coulomb/newton	Piezoelectric Voltage Coefficient 10^{-3} m^2/coulomb	Remarks
• **Ceramics**			
Barium titanate, $BaTiO_3$	34	2	*(continued...)*

Poled Piezoelectric Materials	Piezoelectric Coefficient 10^{-12} coulomb/newton	Piezoelectric Voltage Coefficient 10^{-3} m^2/coulomb	Remarks
Lead niobate, $PbNb_2O_6$	67	34	
Lead zirconate titanate, Pb(Ti, Zn)O_3, PZT	20-50	2-9	
Sodium potassium niobate, (Na,K)NbO_3	40	10	
• **Composites**			
Stycast composite with 25% PZT, by volume	32	25	Under hydrostatic pressures
Spurr composite with 25% PZT, by volume	66	52	
Flexible 33 composite (PZT/$PbTiO_3$)	100	300	
Piezo-rubber	14-48	39-111	

13.5 Application Aspects of Piezoelectric Composites

Merits of piezoelectric composites as electroelastic transducers are:

- Large piezoelectric coefficient (*d* or *g*)
- High electromechanical coupling
- Controllable acoustic impedance
- High sensitivity and compact impulse response
- Complex shape(s) facilitating focused (ultrasonic) excitation reception
- Low cross-talk between electrode arrays
- Low density and mechanical flexibility
- Trade-off optimization in property coefficients of constituent materials
- Fabrication with desirable connectivity (such as thickness node devices)

Typically piezoelectric composite are used in:

- Medical ultrasonic imaging
- Hydrophones

13.6 Theoretical (Design) Considerations

Designing a biphase piezoelectric composite involves the selection of appropriate constituent materials in a proportion such that the end product yields desirable electroelastic characteristics.

The physical properties of the composite material are determined by: (i) The physical properties of the constituent phases; (ii) the volume fractions of the constituents; and, (iii) the structural aspects as decided by the type of connectivity.

Series and parallel arrangements: In a simple diphasic arrangement involving lamellar disposition of the constituents, two types of models, namely, series connection and parallel connection are considered normally (Figure 13.7). These are illustrated in Figures 13.7 corresponding to 3-3 connectivity.

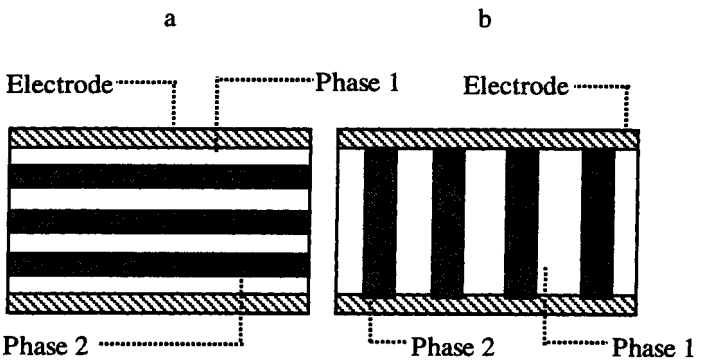

Figure 13.7 Lamellar diphase composite structures interposed between a set of electrodes. a. Series layups of alternate phase 1 (piezoelectric) and phase 2 (nonpiezoelectric) materials; b. Parallel stacking of phase 1 and phase 2 materials.

The effective piezoelastic coefficient (d_{33}) and effective piezoelectric voltage coefficients of series arrangement are given below:

Effective piezoelectric coefficient:

$$(\bar{d}_{33})_{eff} = \frac{v_1(d_{33})_1(\varepsilon_{33})_2 + v_2(d_{33})_2(\varepsilon_{33})_1}{v_1(\varepsilon_{33})_2 + v_2(\varepsilon_{33})_1} \tag{13.1}$$

Piezoelectric voltage coefficient:

$$(\bar{g}_{33})_{eff} = \left(\frac{d_{33}}{\varepsilon_{33}}\right)_{eff} = \frac{v_1(d_{33})_1}{(\varepsilon_{33})_1} + \frac{v_2(d_{33})_2}{(\varepsilon_{33})_2}$$
$$= v_1(g_{33})_1 + v_2(g_{33})_2 \tag{13.2}$$

Parallel arrangements follow.

Piezoelectric coefficient:

$$(\bar{d}_{33})_{eff} = \frac{v_1(d_{33})_1(s_{33})_2 + v_2(d_{33})_2(s_{33})_1}{v_1(s_{33})_2 + v_2(s_{33})_1} \tag{13.3}$$

Piezoelectric voltage coefficient:

$$(\bar{g}_{33})_{eff} = \frac{v_1(d_{33})_1(s_{33})_2 + v_2(d_{33})_2(s_{33})_1}{[v_1(s_{33})_2 + v_2(s_{33})_1][v_1(\varepsilon_{33})_1 + v_2(\varepsilon_{33})_2]} \tag{13.4}$$

Hydrostatic sensitivity is shown below.

For the parallel connection as specified in Figure 13.7b:

$$(d_h)_{eff} \cong [\frac{v_1(d_{33})_1(s_{33})_2 + v_2(d_{33})_2(s_{11})_1}{v_1(s_{33})_2 + v_2(s_{33})_1}] + 2[v_1(d_{31})_1 + v_2(d_{31})_2] \tag{13.5}$$

where subscripts 1 and 2 indicate phases 1 and 2, respectively; and subscript 33 refers to 3-3 connectivity. Further, the other entities indicated represent:

v : volume fraction
d : piezoelectric coefficient
ε : dielectric permittivity
s : elastic compliance

Generalized formulations to calculate the properties of a 0-3 piezoelectric composite (modified cube model due to Banno and Saito [7]) follow.

Dielectric constants ($\bar{\varepsilon}_{33}$, $\bar{\varepsilon}_{22}$, $\bar{\varepsilon}_{11}$):

$$\bar{\varepsilon}_{33} = a^2\,[a + (1-a)n]^2\,(\varepsilon_{33})_1(\varepsilon_{33})_2/[a(\varepsilon_{33})_2 + (1-a)n\,(\varepsilon_{33})_1] + [1 - a^2\,[a + (1-a)n]](\varepsilon_{33})_2 \tag{13.6}$$

Equations for $\bar{\varepsilon}_{11}$ and $\bar{\varepsilon}_{22}$ can be obtained by substituting ε_{11} and ε_{22} for ε_{33}, ℓ and m for n, respectively, in Equation 13.6.

Elastic constants ($\bar{s}_{33}$, $\bar{s}_{22}$, $\bar{s}_{11}$):

$$1/\bar{s}_{33} = a^2\,[a + (1-a)n]^2/[a(s_{33})_1 + (1-a)n\,(s_{33})_2] + [1 - a^2\,[a + (1-a)n]]/(s_{33})_2 \tag{13.7}$$

Equations for $\bar{s}_{11}$ and $\bar{s}_{22}$ can be can be obtained by substituting s_{11} and s_{22} for s_{33}, ℓ and m for n, respectively, in Equation 13.7.

Poisson's ratio ($\bar{\sigma}_{31}$, $\bar{\sigma}_{32}$, $\bar{\sigma}_{12}$, $\bar{\sigma}_{13}$):

$$\bar{\sigma}_{31} = a^2\,[a + (1-a)n][a\,(s_{33})_1(\sigma_{31})_1 + (1-a)n\,\,(s_{33})_2(\sigma_{31})_2] \\ [[a\,\,(s_{33})_1 + (1-a)n\,\,(s_{33})_2] + [1 - a^2\,\,[a + (1-a)n]](\sigma_{31})_2]^{-1} \tag{13.8}$$

An equation for $\bar{\sigma}_{32}$ can be obtained by substituting σ_{32} for σ_{31} in Equation 13.8.

$$\bar{\sigma}_{12} = a^2 [a + (1-a)\ell] \{a\ (s_{11})_1(\sigma_{12})_1 + (1-a)\ell\ (s_{11})_2(\sigma_{12})_2\}$$
$$[\{a\,(s_{11})_1 + (1-a)\ell\,(s_{11})_2\} + \{1 - a^2[a + (1-a)\ell]\}\,(\sigma_{12})_2]^{-1} \tag{13.9}$$

An equation for $\bar{\sigma}_{13}$ can be obtained by substituting σ_{13} for σ_{12} in Equation 13.9.

Dielectric loss tangent ($tan\ \bar{\delta}_{33}$, $tan\ \bar{\delta}_{22}$, $tan\ \bar{\delta}_{11}$):

$$tan\ \bar{\delta}_{33} = A_1/B_1 \tag{13.10}$$

where

$$A_1 = a^2\,(\varepsilon_{33})_2\{a(\varepsilon_{33})_1(tan\delta_{33})_1 + (1-a)n\,(\varepsilon_{33})_2(tan\delta_{33})_2\}$$
$$\times \{a/(\varepsilon_{33})_1 + (1-a)n/(\varepsilon_{33})_2\} + \{1 - a^2[a + (1-a)n]\}$$
$$\times \{a\,(\varepsilon_{33})_1 + (1-a)n(\varepsilon_{33})_2\}(tan\delta_{33})_2 \tag{13.11a}$$

$$B_1 = a^2\,(\varepsilon_{33})_2\{a(\varepsilon_{33})_1 + (1-a)n(\varepsilon_{33})_2\}\{a/(\varepsilon_{33})_1 + (1-a)n/(\varepsilon_{33})_2\}$$
$$+ \{1 - a^2[a + (1-a)\,n]\}\{a(\varepsilon_{33})_1 + (1-a)n(\varepsilon_{33})_2\} \tag{13.11b}$$

Equations for $tan\ \bar{\delta}_{11}$ and $tan\ \bar{\delta}_{22}$ can be obtained by substituting $tan\ \delta_{11}$ and $tan\ \delta_{22}$ for $tan\ \delta_{33}$, ε_{11} and ε_{22}, for ε_{33}, ℓ and m for n, respectively, in Equation 13.11.

Mechanical loss tangent ($tan\ \bar{\delta}_{m\,33}$, $tan\ \bar{\delta}_{m\,22}$, $tan\ \bar{\delta}_{m\,11}$):

Equations for mechanical loss tangent can be obtained by substituting s for ε, $tan\ \delta_m$ for $tan\ \delta$ in Equation 13.11.

Piezoelectric constants $\bar{d}_{31}$, $\bar{d}_{32}$, $\bar{d}_{12}$, $\bar{d}_{13}$:

$$\bar{d}_{33} = A_2/B_2$$

where

$$A_2 = a^2[a + (1-a)n]^2(S_{33})_2\{a(d_{33})_1(\varepsilon_{33})_2 + (1-a)n(d_{33})_2(\varepsilon_{33})_1\}$$
$$+ \{1 - a^2[a + (1-a)n]\}\{a(S_{33})_1 + (1-a)n\,(S_{33})_2\}$$
$$\times \{a(\varepsilon_{33})_2 + (1-a)n\,(\varepsilon_{33})_1\}(d_{33})_2 \tag{13.12a}$$

$$B_2 = a^2[a + (1-a)n]^2(S_{33})_2\{a(\varepsilon_{33})_2 + (1-a)n(\varepsilon_{33})_1\}$$
$$+ \{1 - a^2[a + (1-a)n]\}\{a(S_{33})_1 + (1-a)n(S_{33})_2\}$$
$$\times \{a(\varepsilon_{33})_2 + (1-a)n(\varepsilon_{33})_1\} \tag{13.12b}$$

$$\bar{d}_{31} = A_3 + B_3 + C_3 \tag{13.13}$$

where

$$A_3 = \{a^2[a + (1-a)n]/[a(\varepsilon_{33})_2 + (1-a)n\,(\varepsilon_{33})_1]\}$$
$$\times \{a(d_{31})_1(\varepsilon_{33})_2[a + (1-a)\ell]/[a((S_{11})_1/\ \bar{S}_{11})$$
$$+ (1-a)\ell(S_{11})_2/\ \bar{S}_{11})]\} + (1-a)n(d_{31})_2(\varepsilon_{33})_1/(S_{11})_2/\ \bar{S}_{11})\} \tag{13.14a}$$

$$B_3 = a^2(1-a)\ell[a + (1-a)\ell](d_{31})_2/[a((S_{11})_1/\ \bar{S}_{11}))$$

$$+ (1-a)\ell((S_{11})_2/\bar{S}_{11})\} \tag{13.14b}$$

$$C_3 = \{(1-a)m/[a + (1-a)m] + a(1-a)\ell\,(1-a)n\} \times (d_{31})_2/((S_{11})_2/\bar{S}_{11}) \tag{13.14c}$$

An equation for $\bar{d}_{32}$ can be obtained by substituting d_{32} for d_{31}, S_{22} for S_{11}, ℓ for m, m for ℓ in Equation 13.13, where volume fraction of phase 1, namely, $(v)_1$ is given by:

$$v_1 = a^3 \tag{13.15}$$

Ceramic piezoelectrics with pores (modified cube model due to Banno and Saito [7]):

$$\bar{d}_{33} = (d_{33})_2 \tag{13.16a}$$

$$\bar{d}_{31} = (d_{31})_2\{1 - a/K_s^{1/3} + (a/K_s^{1/3})(1 - a/K_s^{1/3})/(1 + a^2 K_s^{1/3})\} \tag{13.16b}$$

$$\bar{d}_h = d_{33} + 2d_{31} \tag{13.16c}$$

$$\bar{d}_h/\bar{d}_{33} = 1 - (-2(d_{31})_2/(d_{33})_2)\{1 - a/K_s^{1/3} + (a/K_s^{1/3})(1 - a/K_s^{1/3})/(1 + a^2 K_s^{1/3})\} \tag{13.16d}$$

$$\bar{d}_h/(d_h)_2 = 1 + (-2(d_{31})_2/(d_{33})_2)\{(a/K_s^{1/3}) - (a/K_s^{1/3})(1 - a/K_s^{1/3})\} \times [(1 - (-2(d_{31})_2/(d_{33})_2)]^{-1} \tag{13.16e}$$

$$\bar{\varepsilon}_{33}/(\varepsilon_{33})_2 = 1 - (a/K_s^{1/3})^2\,\{1 - 1/(a((\varepsilon_{33})_2/\varepsilon_0 - 1) + 1)\} \tag{13.16f}$$

where the volume fraction of pore v_1 is a^3 and the notation K_s is a parameter attributed to pore shape of phase 1. When phase 1 pores are cubic or flat tetragonal, K_s becomes unity or less than unity, respectively (Figure 13.8).

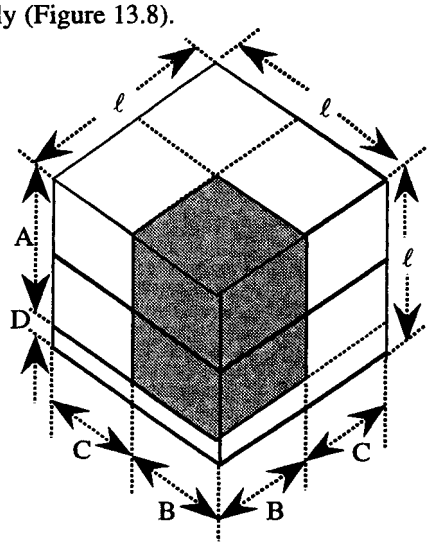

Figure 13.8 Shaped factor of the phase 1 in modified cubes model.
A: a/[a + (1 – a)n].
B: a/[a + (1 – a)m].
C: (1 – a)m/[a + (1 – a)m].
D: (1 – a)n/[a + (1 – a)n].
Shape factor of phase 1: K_s = A/B.

Using K_s and assuming that the relative dielectric constant of the pore is unity, theoretical equations of the dielectric and piezoelectric $\bar{\varepsilon}_{31}$ constants of the porous ceramics are obtained as follows:

$$\bar{\varepsilon}_{33} = (\varepsilon_{33})_2 \left\{ 1 + \frac{1}{a((\varepsilon_{33})_2 - 1)K_s^{2/3} + 1K_s^{2/3} - \frac{a^2}{K_s^{2/3}}} \right\} \tag{13.17a}$$

$$\bar{d}_{31} = (d_{31})_2 \left\{ 1 - \frac{a}{K_s^{1/3}} + \frac{\frac{a}{K_s^{1/3}}\left(1 - \frac{a}{K_s^{1/3}}\right)}{1 - a^2 K_s^{1/3}} \right\} \tag{13.17b}$$

where $(\varepsilon_{33})_2$ and $(d_{31})_2$ are the relative dielectric and piezoelectric constants of the bulk ceramic material, respectively, and a^3 $(= v_1)$ is the volume fraction of the pore.

Binary piezoelectric composite with a continuous dielectric host medium and piezoelectric ellipsoidal inclusions: An example of this system refers to a mixture of lead zirconate titanate (PZT) particles dispensed in a poly-vinylidene fluoride (PVDF) receptacle. Relevant formulations to calculate the effective mixture parameters follow.

Dielectric constant:

$$\varepsilon_{eff} = \varepsilon \left[1 + [n\theta(\varepsilon_2 - \varepsilon_1)]/[n\varepsilon_1 + (\varepsilon_2 - \varepsilon_1)(1 - \theta)] \right] \tag{13.18}$$

where $n = 4\pi/m$ is a parameter attributed to the shape of the ellipsoidal particles and θ is the volume fraction of the ellipsoidal particles; and

$$m = \int_0^\infty du/[(a^2+u)\beta_u]$$

$$\beta_u = \{[(a^2 + u)(b^2 + u)(c^2 + u)]^{1/2}\}/2\pi abc$$

a,b,c : Semiaxial lengths of the ellipsoidal particles.
ε_1 : Dielectric permittivity of the host medium.
ε_2 : Dielectric permittivity of the ellipsoidal inclusions.

Piezoelectric constant:

$$d_{eff} = \theta \alpha G d_2 \tag{13.19}$$

where

$$G = n\left\{(\varepsilon_2/\varepsilon_1) - 1 + n + (n-1)[(\varepsilon_2/\varepsilon_1) - 1]\theta\right\}/$$
$$\left\{[(\varepsilon_2/\varepsilon_1) - 1 + n]^2 + [(\varepsilon_2/\varepsilon_1) - 1][(n-1)^2 - (\varepsilon_2/\varepsilon_1)]\theta\right\}$$

α = Poling ratio
d_2 = Piezoelectric constants of the piezoelectric particles.

Elastic constant:

$$E_{eff} = E_1 \{1 + [\theta (E_2 - E_1)]/[E_1 + n'(E_2 - E_1)(1 - \theta)]\} \tag{13.20}$$

E : Young's modulus
1,2 : Subscripts to denote the host medium and the dispensed particles
n' : $(1/3)\ (1 + \sigma)/(1 - \sigma)$
σ = Poisson's ratio of the host medium

Neuromimetic model [8]: In [8], the author and Park had developed a neuromimetic model to describe the electroelastic synergism in piezoelectric composites. That is, the electroelastic response of a piezoelectric composite material (constituted by piezoelectric particulate dispersions in a nonpiezoelectric receptacle) is emulated analogous to the collective response of randomly interconnected neurons. By comparing the stochastic aspects of both systems, the effective parameters of the piezoelectric composite are deduced. Theoretical results on the effective piezoelectric coefficients of two types of test composites are compared with the relevant available experimental data. The neuromimetic concept envisaged facilitates a understanding of the behavior of advanced piezoelectric composites *vis-a-vis* the constituent materials of such composites. Relevant study also refers to the effects of the size, shape, volume fraction, and orientation of the inclusions and the characteristics of the host medium in deciding the net electroelastic response of the composite. The strategy presented in [8] indicates a neural network approach in studying such composites constituted by randomly dispersed interacting inclusions.

On the basis of the above considerations, the theoretic formulations obtained are summarized below.

For dispension of shaped piezoelectric particles with arbitrary orientational dispositions, the effective piezoelectric coefficient is given by :

$$d_{eff} = \{(d_{eff})_p\}^u / \{(d_{eff})_s\}^{u-1} \tag{13.21}$$

where

$$(d_{eff})_p = \{d_2/[1 + \frac{s_1(1-\theta)}{s_2\ \ \theta}] + d_2/[1 + \frac{s_2\ \ \theta}{s_1(1-\theta)}]\}$$

and 1, 2 are subscripts denoting the media 1 and 2, respectively. Further,

d : Piezoelectric coefficient
ε : Dielectric permittivity
θ : Volume fraction of medium 1
s_1 : Elastic compliance
u $= (u_S + u_G)^{1/2}$
u_G : Order parameter decided by the particulate shape; $1/3 \le u_G\ (a/b) \le 1$
u_S : Order parameter decided by the particulate (an isotropic) spatial orientation
$1/3 \le u_S \le 1$
a/b : Ratio of semiaxial lengths of the spheroidal inclusions

$$u_G = [1 - \frac{m^R}{\sum_{\ell=0}^{R} m_o^\ell}]/[1 - \frac{m_\infty^R}{\sum_{\ell=0}^{R} m_o^\ell}]$$

R = Nearest integer of [0.5 + 0.5 (a/b)], if $a/b > 1$
= Nearest integer of [0.5 + 0.5 (b/a)], if $a/b < 1$

m $= e^2[(1 - \sqrt{1 - e^2}\arcsin(e)/e)^{-1}$; (Sillars' shape parameter)

e : Particulate eccentricity

$$= \begin{cases} [1 - (b/a)]; a > b \\ [(a/b) - 1]; a < b \end{cases}$$

m_o = 3

m_∞ = 1

u_S = $\langle \cos^2\alpha \rangle$, where α refers to the angle of preferential orientation (or degree of anisotropicity) in the spatial dispositions of the particles.

α = 1/3: Totally isotropic random dispension of the particulate inclusions.
= 1: Totally anisotropic (parallel or antiparallel arrangement of the particles).

13.7 Experimental Data on Piezoelectric Composites

Figures 13.9–13.16 depict typically the variations of the characteristics of piezoelectric composites with respect to temperature, volume fraction of piezoelectric material, poling conditions and adding of another piezoelectric materials.

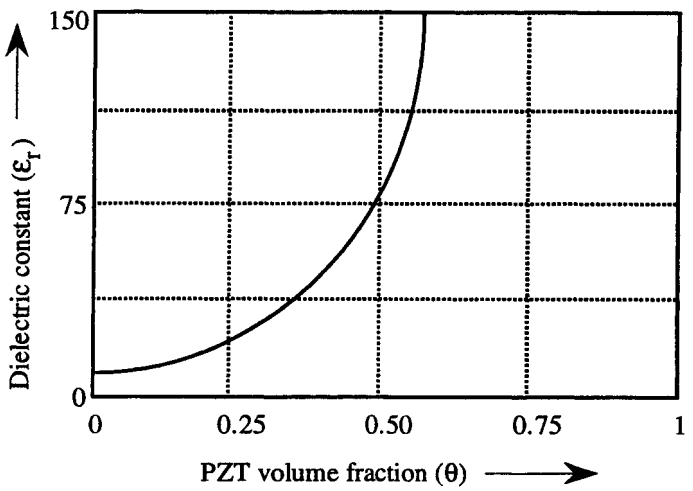

Figure 13.9 Dielectric constant (ε_r) *versus* volume fraction (θ) of PZT content in a piezoelectric composite at room temperature.

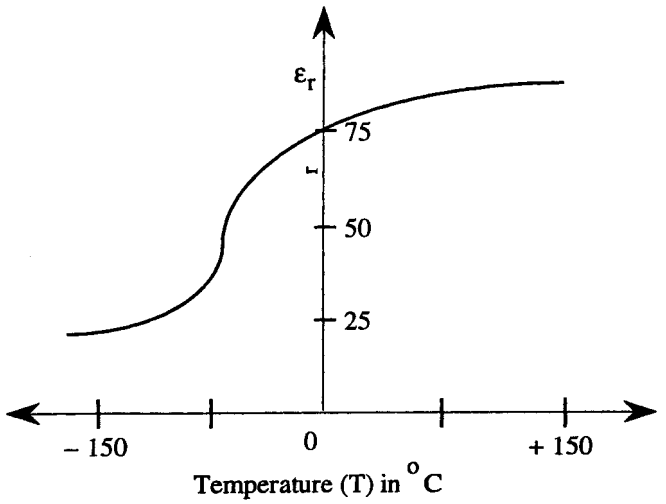

Figure 13.10 Temperature (T) *versus* dielectric constant (ε_r) of a PZT-included piezoelectric composite. PZT volume fraction (θ) ≈ 0.5.

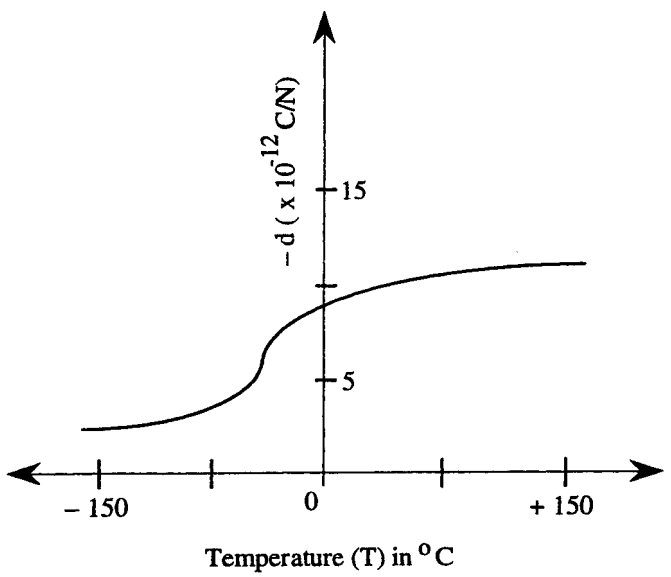

Figure 13.11 Temperature (T) *versus* piezoelectric coefficient (d) of a PZT-included piezoelectric composite. Volume fraction of PZT (θ) ≈ 0.5.

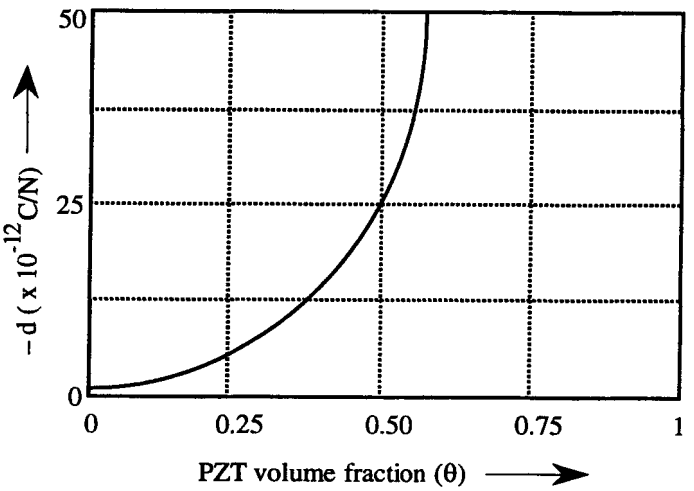

Figure 13.12 PZT volume fraction (θ) *versus* piezoelectric coefficient (d) of a PZT-included piezoelectric composite at room temperature.

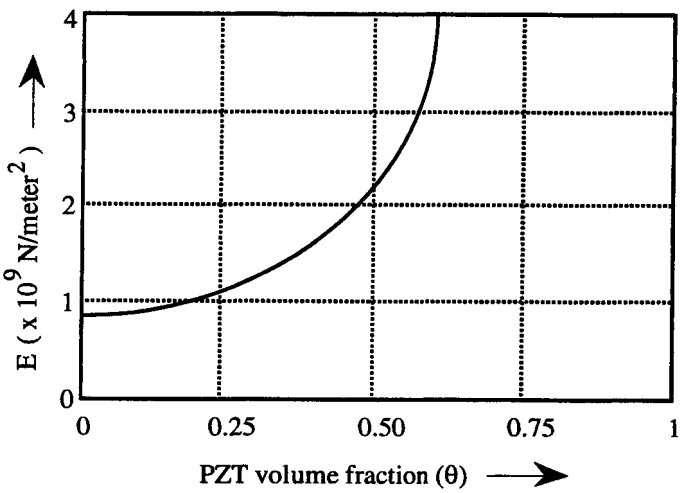

Figure 13.13 PZT volume fraction (θ) *versus* elastic modulus (Young's modulus E) of a PZT-included piezoelectric composite at room temperature.

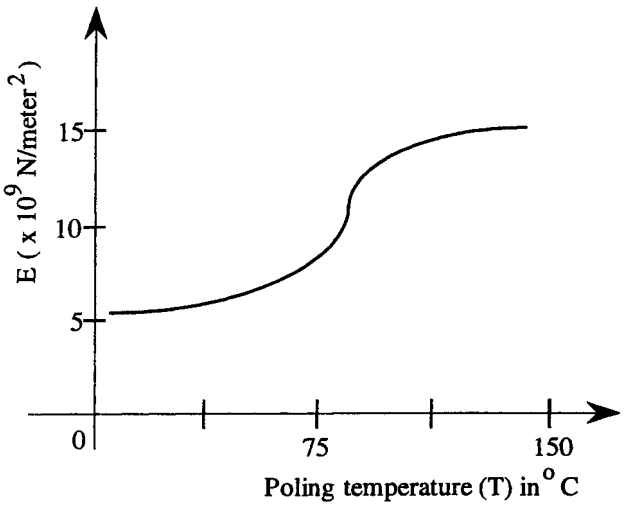

Figure 13.14 Poling temperature (T) *versus* piezoelectric coefficient (d) of PZT-included piezoelectric composite. (PZT volume fraction $\theta \approx 0.5$; poling electric field (ξ): 10×10^9 volt/meter; Duration of poling: 120 minutes.)

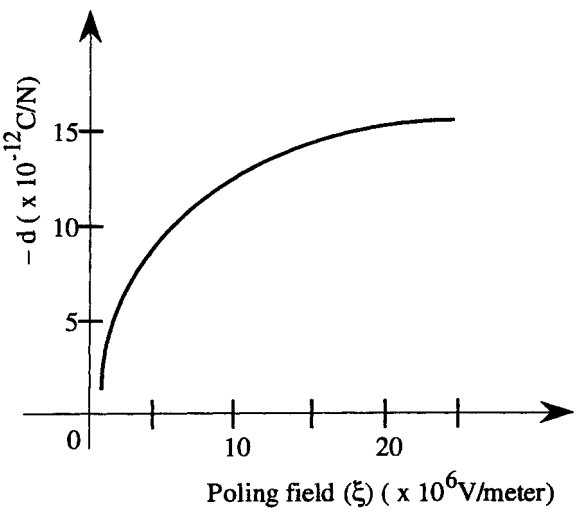

Figure 13.15 Poling field (ξ) *versus* piezoelectric coefficient (d) of a PZT-included piezoelectric composite. ($\theta \approx 0.5$; Poling temperature: 100°C; and poling time: 120 minutes.)

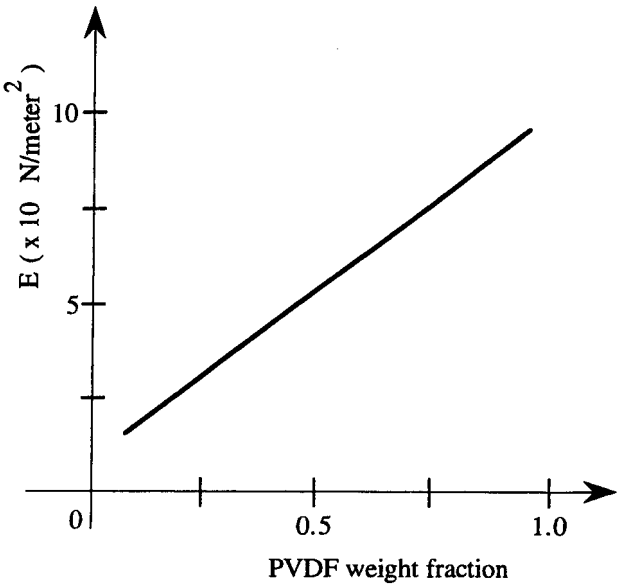

Figure 13.16 Weight fraction of PVDF *versus* Young's modulus (E) of a PVDF-based piezoelectric composite at room temperature. (Volume fraction of PVDF (θ) $\approx$ 0.7.)

References

[1] J. Wolak: Dielectric behavior of 03-type piezoelectric composites. IEEE Trans. Elec. Insulation, vol. 28(1), 1993: 116-121.

[2] H. Zewdie and F. Brouers: Theory of ferroelectric polymer-ceramic composites. J. Appl. Phys., vol. 68, 1990: 713-718.

[3] M. Chino et al.: Microwave absorbers using ferroelectric/rubber composite structure and their evaluation. Ferroelectrics, vol. 93, 1989: 67-71.

[4] H. Banno: Theoretical equations for dielectric, piezoelectric and elastic properties of flexible composite consisting of polymer and ceramic powder of two different materials. Ferroelectrics, vol. 95, 1989: 111-115.

[5] H. Banno: Recent progress in science and technology of flexible piezoelectric composite in Japan, Proc.7th International Symp. on Application of Ferroelectrics, pp. 67-72.

[6] W. A. Smith: The role of piezocomposites in ultrasonic transducers, Proc. 1989 Ultrasonics Symp., pp. 755-766.

[7] H. Banno and S. Saito: Piezoelectric and dielectric properties of composites of synthetic rubber and $PbTiO_3$ or PZT. Japanese J. Appl. Phys., vol. 22 (Supplement 22-2), 1983: 67-69.

[8] P. S. Neelakanta and J. C. Park: Neuromimetic model of electroelastic synergism in piezoelectric composites. Biomimetics, vol. 2(1), 1993: 33-56.

[9] A. A. Shanlov, W. A. Smith and R. Y. Ting: Modified lead-titanate/polymer composites for hydrophone applications. Ferroelectrics, vol. 93, 1989: 177-182.

[10] D. P. Skinner, R. F. Newham and L. E. Cross: Flexible composite transducers. Mat. Res. Bull., vol. 13, 1978: 599-607.

[11] R. E. Newham, D. P. Skinner and L. E. Cross: Connectivity and piezoelectric-pyloelectric composites. Mat. Res. Bull., vol. 13, 1978: 525-536.

[12] Data sheet: NTK Piezoelectric Rubber. (NTK Technical Ceramic Division), NGK Spark Plug Co. Ltd., Mihuho, Nagoya, 467 Japan).

Defining Terms

Connectivity: Refers to the pattern in which the diphasic or multiphasic constituents in a anisotropic composite are self-connected in zero, one, two, or three dimensions.

Dielectric constant: Relative permittivity of the medium; in the anisotropic case as in piezoelectric composites, is a tensor parameter.

Dielectric loss tangent: Depicts the lossy nature of a dielectric (monolithic or composite) material.

Dice and fill process: Process in which deep grooves are cut in a piezoelectric ceramic and grooves are filled with a polymer to realize a piezoelectric composite.

Elastic constants: Young's bulk or shear modulii of elasticity tensor parameters; in anisotropic materials such as piezoelectric composites.

Hydrophone: An underwater acoustical transducer.

Laminated piezoelectric composite: Alternate stacking of piezoelectric and nonpiezoelectric materials.

Neuromimetic model: Behavior of a material mimicking the neuronal state transitional characteristics.

Piezoelectric composites: A combination of a piezoelectric-ceramic and/or a polymer and a nonpiezoelectric polymer.

Piezoelectric constant: Expresses the polarization along a particular direction produced by an elastic strain in a monolithic or composite piezoelectric material.

Piezoelectric coefficient (d or g): The piezoelectric stress per charge induced in a monolithic and/or composite piezoelectric material.

Poling field: Minimum electric field (kV/m) required to polarize a monolithic or composite piezoelectric material.

Poling temperature: Temperature at which piezoelectric poling is done.

Replication process (replamineform process): Fabric templates consisting of woven carbon fibers impregnated with PZT and subsequent heat-treatment burns out carbon, leaving behind PZT.

Rod composites: Rod-like piezoelectric material embedded in a polymer or ceramic with 1-3 connectivity.

Rubber piezoelectric composites: Flexible piezoelectric composites constituted by piezoelectric inclusions in a rubber material.

Ultrasonic imaging: Using ultrasonic transducers, reflection of ultrasonic energy from a body which is processed to "image" the body irradiated with ultrasonics.

Woven ceramic/polymer composites: Piezoelectric composites with interwoven dispersion of piezoelectric inclusions obtained by refraction or replamineform process.

Table 13.2 Comparison of Physical Properties of Typical Piezoelectric Composites

Materials	Parameters									
	K_{33}	d_{33} (pc/N)	d_h (pc/N)	g_h ($\times 10^{-3}$ Vm/N)	$d_h g_h$ ($\times 10^{-5}$ m^2)	d_{31} (pc/N)	ε_r	tanδ	PF* KV/m	Density
PZT single phase	1760	450	42	2.7	113	–204				
PZT 1-3 composite	22	217	10	52	50-520	–83				
PZT 1-3-0 composite 20% void	110	270	220	220	228	–25				
PZT 1-3-0 composite 30% void	24 - 25	225	60-100	295-446						
PZT 1-3-0 composite 40% void	110	310	284	285	94	–13				
PZT plus polymer (Spurr epoxy)		25	6	18	108		38	0.017	66	
PZT plus Eccogel		90	30	108	2100		48	0.25	40	
Piezo-rubber (NTK)		34-56	17-44	45-124	765-5084	–2.5- –18.5	43-45 (ε_{33})	2 - 6		5.3-5.9
PZT 3-3 composite with silicone rubber		100		300 (g_{33})			40			3.3
Calcium modified lead titanate plus polymer (Spurr epoxy or Stycast)		49-59	32-25	66-52	2100- 1300	–8.5- –17.0			54-55	

*PF: Poling Field.